NAVAL POSTGRADUATE SCHOOL

MONTEREY, CALIFORNIA

THESIS

THERMAL MODELING OF GAN HEMTS ON SAPPHIRE AND DIAMOND

by

Roman Peter Salm III

December 2005

Thesis Advisor:	Todd R. Weatherford
Second Reader:	Andrew A. Parker

Approved for public release; distribution is unlimited

THIS PAGE INTENTIONALLY LEFT BLANK

REPORT DOCUMENTATION PAGE			Form Approved OMB No. 0704-0188
Public reporting burden for this collection of information is estimated to average 1 hour per response, including the time for reviewing instruction, searching existing data sources, gathering and maintaining the data needed, and completing and reviewing the collection of information. Send comments regarding this burden estimate or any other aspect of this collection of information, including suggestions for reducing this burden, to Washington headquarters Services, Directorate for Information Operations and Reports, 1215 Jefferson Davis Highway, Suite 1204, Arlington, VA 22202-4302, and to the Office of Management and Budget, Paperwork Reduction Project (0704-0188) Washington DC 20503.			
1. AGENCY USE ONLY *(Leave blank)*	**2. REPORT DATE** December 2005	**3. REPORT TYPE AND DATES COVERED** Master's Thesis	
4. TITLE AND SUBTITLE: Thermal Modeling of GaN HEMTs on Sapphire and Diamond			**5. FUNDING NUMBERS**
6. AUTHOR(S) Roman Peter Salm III			
7. PERFORMING ORGANIZATION NAME(S) AND ADDRESS(ES) Naval Postgraduate School Monterey, CA 93943-5000			**8. PERFORMING ORGANIZATION REPORT NUMBER**
9. SPONSORING /MONITORING AGENCY NAME(S) AND ADDRESS(ES) N/A			**10. SPONSORING/MONITORING AGENCY REPORT NUMBER**
11. SUPPLEMENTARY NOTES The views expressed in this thesis are those of the author and do not reflect the official policy or position of the Department of Defense or the U.S. Government.			
12a. DISTRIBUTION / AVAILABILITY STATEMENT Approved for public release; distribution is unlimited			**12b. DISTRIBUTION CODE**

13. ABSTRACT (maximum 200 words)

Wide bandgap semiconductors have entered into Naval radar use and will eventually replace vacuum tube and conventional solid-state amplifiers for all modern military radar and communications applications. Gallium Nitride (GaN) High Electron Mobility Transistors (HEMTs) are on the leading edge of wide bandgap technology and have the performance characteristics to dominate in high power – high bandwidth applications. The Defense Advanced Research Projects Agency (DARPA), Office of Naval Research (ONR) and Missile Defense Agency (MDA) are all sponsoring research projects to apply wide bandgap technology. This thesis studies the effects of changing the substrate material of an existing GaN HEMT from sapphire to diamond through the use of commercially available Silvaco software for modeling and simulation. The unparalleled thermal properties of diamond are expected to dramatically decrease device temperatures and increase component lifetimes and reliability.

14. SUBJECT TERMS High Electron Mobility Transistor, Gallium Nitride, Heterostructure, Diamond Substrate			**15. NUMBER OF PAGES** 71
			16. PRICE CODE
17. SECURITY CLASSIFICATION OF REPORT Unclassified	**18. SECURITY CLASSIFICATION OF THIS PAGE** Unclassified	**19. SECURITY CLASSIFICATION OF ABSTRACT** Unclassified	**20. LIMITATION OF ABSTRACT** UL

NSN 7540-01-280-5500 Standard Form 298 (Rev. 2-89)
Prescribed by ANSI Std. 239-18

THIS PAGE INTENTIONALLY LEFT BLANK

Approved for public release; distribution is unlimited

THERMAL MODELING OF GAN HEMTS ON SAPPHIRE AND DIAMOND

Roman P. Salm III
Lieutenant, United States Navy
B.S., University of Wisconsin, 1997

Submitted in partial fulfillment of the
requirements for the degree of

MASTER OF SCIENCE IN ELECTRICAL ENGINEERING

from the

NAVAL POSTGRADUATE SCHOOL
December 2005

Author: Roman Peter Salm III

Approved by: Todd R. Weatherford
Thesis Advisor

Andrew A. Parker
Second Reader

Jeffrey B. Knorr
Chairman, Department of Electrical and Computer Engineering

THIS PAGE INTENTIONALLY LEFT BLANK

ABSTRACT

Wide bandgap semiconductors have entered into Naval radar use and will eventually replace vacuum tube and conventional solid-state amplifiers for all modern military radar and communications applications. Gallium Nitride (GaN) High Electron Mobility Transistors (HEMTs) are on the leading edge of wide bandgap technology and have the performance characteristics to dominate in high power – high bandwidth applications. The Defense Advanced Research Projects Agency (DARPA), Office of Naval Research (ONR) and Missile Defense Agency (MDA) are all sponsoring research projects to apply wide bandgap technology. This thesis studies the effects of changing the substrate material of an existing GaN HEMT from sapphire to diamond through the use of commercially available Silvaco software for modeling and simulation. The unparalleled thermal properties of diamond are expected to dramatically decrease device temperatures and increase component lifetimes and reliability.

THIS PAGE INTENTIONALLY LEFT BLANK

TABLE OF CONTENTS

THIS PAGE INTENTIONALLY LEFT BLANK

LIST OF FIGURES

THIS PAGE INTENTIONALLY LEFT BLANK

LIST OF TABLES

THIS PAGE INTENTIONALLY LEFT BLANK

ACKNOWLEDGMENTS

I would like to thank Prof. Todd Weatherford for his dedication and guidance during the work on this thesis. Dr. Petra Specht and her staff at U.C. Berkeley also deserve acknowledgement for beginning and continuing their work fabricating and analyzing compound heterostructures. Jerry Zimmer and his team at SP3 Diamond Technologies deserve recognition for their excellent support and for providing the substrate material. All of their efforts made this research possible. My wife and children also deserve more gratitude than I can fathom for supporting me during these many months of hard work.

THIS PAGE INTENTIONALLY LEFT BLANK

EXECUTIVE SUMMARY

A computer model of Gallium Nitride (GaN) High Electron Mobility Transistors (HEMTs) has been developed for the purpose of designing and modifying high power – high frequency amplifiers. GaN HEMT and other wide bandgap semiconductor devices are being investigated for applications in communications and military radar. Using GaN technology over currently fielded Gallium Arsenide (GaAs) could result in a tenfold increase in power density at identical frequencies. GaN devices offer superior material properties for high power – high bandwidth applications, especially at high voltages where current GaAs technology is unsuitable. This model includes thermal effects and considers using a diamond substrate for thermal management. Diamond has the highest thermal conductivity of any known substance and can be easily grown on large wafers. Current HEMTs achieve around 12 W/mm with gate geometries similar to those modeled here. Device performance in excess of 20 W/mm and an increase in component lifetimes by several orders of magnitude may be possible if a high thermal conductor such as diamond can be utilized in a GaN HEMT to reduce channel temperatures. This would lower system downtime, reduce system lifecycle costs and increase overall system performance and warfighting capability.

The Silvaco software, a physics-based modeling program, was utilized to model and simulate an $Al_{0.28}Ga_{0.72}N$/GaN HEMT on a sapphire and finally a diamond substrate. The model is based on an actual device built and tested while completing a doctoral dissertation by Suzie Tzeng at the University of California (UC) – Berkeley. The model proved capable of closely matching the expected IV characteristics after numerous model parameters were adjusted.

A three-dimensional thermal model of the device on sapphire was created and tested to be electrically similar to the two-dimensional model. Thermal characteristics and localized heating effects can be observed while the model was biased at typical operating conditions. A two-dimensional thermal comparison between sapphire and diamond substrates with devices of otherwise identical structure was conducted. Possibilities for improving the model are discussed and recommended for future research.

THIS PAGE INTENTIONALLY LEFT BLANK

I. INTRODUCTION

A. BACKGROUND

Next generation communications and radar systems of our Navy require more capability in terms of bandwidth and power in continued support of the Sea Power 21. Radio Frequency (RF) amplifier technology is at the heart of every radar and communication system. In the Navy, this technology has been dominated by vacuum tubes/traveling wave tubes for years. Modern demands of bandwidth, power, space, weight, cost, efficiency and reliability have all but exhausted the capabilities of the venerable vacuum technology.

The solid-state technology, specifically the semiconductor amplifier, is found in thousands of commercial communication devices such as cellular phones, wireless computers and commercial vehicle navigation systems. Next-generation radar and communications devices require compound semiconductors for more bandwidth and higher power. Compound semiconductors such as Gallium Nitride (GaN), Gallium Arsenide (GaAs) and Silicon Carbide (SiC) show the most promise. GaAs technology is currently fielded by the Department of Defense (DoD) in low power receivers and SiC will be instrumental as we as a Navy transition to electric drive propulsion. The continued improvements made in GaN technology make its widespread use in next generation Naval radar and communication systems inevitable. High power – high bandwidth amplifiers based on solid-state technology are currently being developed by other DoD agencies for systems to be fielded in the near future.

Attribute	Si	GaAs	SiC	GaN
Energy Gap (eV)	1.11	1.43	3.2	3.4
Breakdown E-Field (V/cm)	6.0×10^5	6.5×10^5	3.5×10^6	3.5×10^6
Saturation Velocity (cm/s)	1.0×10^7	2.0×10^7	2.0×10^7	2.5×10^7
Electron Mobility (cm2/V-s)	1350	6000	800	1600*
Thermal Conductivity (W/cmK)	1.5	0.46	3.5	1.7
Heterostructures	SiGe/Si	AlGaAs/GaAs InGaP/GaAs AlGaAs/InGaAs	None	AlGaN/GaN InGaN/GaN

* Typical two-dimensional electron gas mobility for AlGaN/GaN heterostructures.

Table 1. Material Properties of Common Semiconductors [1]

Material properties of several semiconductors, summarized in Table 1, clearly show that GaN shows great promise for use in high power microwave applications. Its wide bandgap allows for lower leakage and higher device breakdown voltages; the heterostructure capability decreases noise; and higher saturation velocity and breakdown field enable higher frequencies. GaN is among the most promising of known semiconductors when searching for highest power and highest bandwidth capability.

B. RELATED WORK

Previous NPS efforts have used Silvaco models to represent GaN HEMT devices [2, 3]. These works focused on the piezoelectric effect of GaN and AlGaN and how to implement the effect into a software model. Naval Research Laboratories (NRL) had initially supplied data from actual devices for further study to NPS. This work gleans some of the recommendations from the earlier research to incorporate thermal simulation capabilities of the Silvaco software suite to improve on the modeling an actual device. The real impetus of this work began with Jerry Zimmer and SP3 Diamond Technologies. SP3 approached NPS with high-quality polycrystalline diamond and a query as to its most promising use. Professor Weatherford provided the direction necessary to attempt to substitute diamond as a substrate material for GaN HEMTs grown at UC – Berkeley and model it to further enhance GaN HEMT performance. SP3, UC – Berkeley and NPS have pursued research funding through MDA solicitations of innovative wide bandgap semiconductor technology for RF application.

C. OBJECTIVES

The purpose of this research is to create a model that most closely mimics the actual electrical, physical and thermal characteristics of the device created by UC - Berkeley to allow for simulation of three-dimensional thermal characteristics. With a complete and accurate device model, optimization and testing techniques can be used to guide the direction of future HEMT efforts. Understanding the thermal and electrical properties will allow for optimization of the GaN transistor structure, the geometry of the diamond substrate and prediction of thermal conductivity across layer interfaces. If a high thermal conductor such as diamond can be utilized in a GaN HEMT to reduce channel temperatures, both improved device performance and most importantly

component lifetimes may be increased by several orders of magnitude. This would lower system downtimes, reduce system lifecycle costs and increase overall system performance and warfighting capability.

THIS PAGE INTENTIONALLY LEFT BLANK

II. HEMT FUNDAMENTALS

A. HIGH ELECTRON MOBILITY TRANSISTOR

A HEMT is field-effect transistor that operates very similar to a Metal-Semiconductor Field Effect Transistor (MESFET). Electron flow across the carrier channel from source to drain is modulated by changing gate voltage. The main difference between a MESFET and a HEMT is the device structure. HEMTs use different compounds grown in layers to optimize and extend the performance of the MESFET. The different layers form heterojunctions [4]. Figure 1 shows the basic HEMT structure.

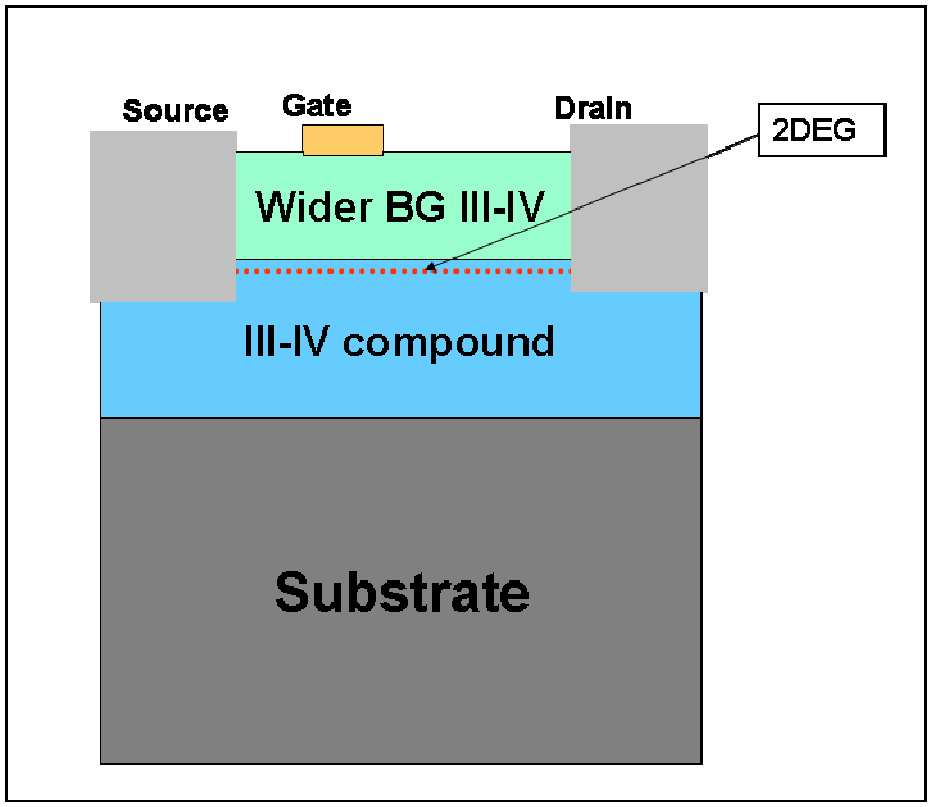

Figure 1. Basic Diagram of a HEMT

The first HEMT was invented in 1979 by Takashi Mimura. At that time, conventional thinking was that the only way to get electrons to move through a semiconductor was to add n-type impurities to create free electrons. This convention, still applied in nearly all semiconductor technology, causes the electrons to 'slow down'

because of collisions with the same impurities used to create the free electrons. The HEMT is the exception to the rule. By exploiting the characteristics of a heterojunction, the bandgap differences between two materials create a quantum well in one dimension. The quantum well produces a 2-dimensional electron gas (2DEG) on one side of the boundary where electrons experience a substantial reduction in scattering effects.

B. GALLIUM NITRIDE

1. Material Properties

The large bandgap and high dielectric strength of Gallium Nitride make it an ideal semiconductor for high-power devices such as diodes, amplifiers and switches. The bandgap is the major property contributing to its low leakage current. These characteristics make GaN ideal for creating smaller devices capable of higher operating frequencies and handling more power and voltage. GaN is among the most promising compound semiconductors when considering material for high-power, high-frequency amplification. The ability to function in a heterostructure configuration coupled with a high breakdown field make GaN far superior to GaAs or SiC for use in millimeter wave, low-noise, high-power applications. As the manufacture of GaN continues to improve, defect densities will decrease; further increasing reliability and device noise characteristics.

2. GaN Challenges

Current GaN limitations stem from a variety of sources. Most notable is the absence of a native substrate. Unlike silicon, GaN does not exist in a pure form in nature. GaN must be 'grown' in layers an atom at a time through chemical vapor deposition or electron beam epitaxy. Additionally, the processes used to create GaN material in quantity leave many impurities and these impurities create problems for device production, performance and reliability. To take full advantage of the material properties, GaN microwave devices are made increasingly smaller and the defects induced by impurities have made device reliability and performance quite variable. Methods to increase GaN HEMT performance have speculated that hydrogen passivation into epitaxial layers through a variety of plasma induced techniques during processing may make devices less susceptible to hot electron damage or mitigate the damage as it occurs during device degradation [5]. Defects introduced during growth of the AlGaN

layer, high temperature deposition of contacts and other device building processes are all compounded by the impurity levels in the original GaN material. Ongoing efforts to determine device failure mechanisms and increase purity levels are necessary for GaN devices to become more reliable.

Popular substrate materials currently used for GaN HEMTs include sapphire, Silicon Carbide (SiC), silicon and Aluminum Nitride (AlN). Each substrate choice has been proven with individual successes and challenges. At the outset of GaN research, sapphire (Al_2O_3) had been a popular choice for substrate material due to its high melting point and ready availability. GaN purity levels are affected during vapor growth by the interaction of hydrogen gas and the oxygen in sapphire, creating unwanted defects. As GaN research was able to achieve higher power levels, the thermal conductivity of sapphire has also been a limiting factor [6]. To mitigate defects due to oxygen, pure silicon has been used quite successfully as a substrate material for GaN HEMTs. Thermal conductivity is similar to that of GaN. High purity silicon and large wafer sizes are readily available due to its popularity. However, lattice mismatch requires the use of a nucleation or boundary layer, further increasing the channel distance from the thermal management substrate [1]. SiC has been a popular choice for high-power HEMT use providing a much higher thermal conductivity. Defects in the GaN caused by micropipe and other defects in SiC have made GaN layer growth difficult as the crystal structure struggles to maintain uniformity during the growth process [6]. AlN is often used as a nucleation layer between silicon based substrates and GaN to allow for lattice matching during the growth process. As a free standing substrate, AlN has shown some promise as a GaN HEMT substrate choice but its thermal conductivity is only equal to that of sapphire.

The thermal conductivity of GaN is a challenge to overcome. Table 2 shows several popular semiconductor device materials and their thermal conductivities. The tabulated values were used in the device model. While able to support high temperature operation, GaN by itself is unable to sufficiently remove the heat generated during intended device operation. Increased thermal resistance and shortened device component lifetimes are just two of the many undesired effects of high device temperatures. Removing the heat generated during operation could dramatically increase device

performance, reliability and lifetime. Substrate selection for GaN HEMTs has primarily focused on sapphire and SiC due to their availability and ease of growing GaN onto these substrates. This work hopes to present diamond, the best thermal conductor known, as an option for GaN HEMT devices and the likely benefits if such a substrate solution is feasible.

Substrate	Thermal Conductivity (W/cm·K)
Diamond	10
Sapphire	1.7
GaN	1.3
AlN	1.7
SiC	4.9
Si	1.5

Table 2. Substrate Thermal Conductivities

Thermal boundary resistance is another heat related challenge once a substrate material is selected. The boundary between GaN and the substrate does not perfectly conduct heat energy away from the device. The very tight covalent structure is missing at the interface so this thermally "high" resistance point will retard the heat flux generated above it providing a high temperature gradient locally at interface. Self-heating effects have been observed in both GaN on SiC and GaN on sapphire. The GaN boundary layers have been theoretically estimated to dissipate power at 12 W/mm for GaN-on-SiC and 2.5 W/mm for GaN-on-sapphire [7]. The GaN-diamond thermal boundary resistance has yet to be estimated but if the interface quality is similar to the GaN-on-SiC, GaN-on-diamond should provide dissipation in excess of 20 W/mm due to the thermal conductivity value of diamond being more than twice that of SiC.

C. STATE-OF-THE-ART GAN FETS

Power and microwave devices for use in the commercial or military market share common needs listed in the first column of Table 3. The second column lists the Enabling Feature of GaN-based devices to fulfill the need.

Need	Enabling Feature	Performance Advantage
High Power/Unit Width	Wide Bandgap, High Field	Compact, Ease of Matching
High Voltage Operation	High Breakdown Field	Eliminate/Reduce Step Down
High Linearity	HEMT Topology	Optimum Band Allocation
High Frequency	High Electron Velocity	Bandwidth, μ-Wave/mm-Wave
High Efficiency	High Operating Voltage	Power Saving, Reduced Cooling
Low Noise	High gain, high velocity	High dynamic range receivers
High Temperature Operation	Wide Bandgap	Rugged, Reliable, Reduced Cooling
Thermal Management	SiC Substrate	High power devices with reduced cooling needs
Technology Leverage	Direct Bandgap: Enabler for Lighting	Driving Force for Technology: Low Cost

Table 3. Competitive Advantages of GaN Devices [8]

The most significant benefits of GaN are highlighted in Table 3. For example, "the high power per unit width translates into smaller devices that are not only easier to fabricate but also offer much higher impedance" [8]. This feature allows for easier source and load matching to existing power supplies, transmission lines and antennas. Current GaAs amplifying devices require impedance and voltage matching transformers, which add cost, complexity and weight where GaN devices can operate at higher voltages and do not require the extras.

Recent advances in GaN HEMT technology have shown rapidly increasing device performance. In the late 1990's, GaN HEMTs on sapphire were tested at power ratings around 10 W/mm but experienced almost instantaneous power and noise degradation. The negative effects of poor thermal conductivity and growth related defects of sapphire saw SiC emerge as the substrate of choice soon thereafter. In 2002 reported HEMT power outputs on SiC achieved merely single digit W/mm ratings [8]. Research in 2003 saw power levels of around 14 W/mm as passivation methods and growth techniques improved [9]. Field plate gate fabrication methods have been able to increase device performance to a healthy 32 W/mm. The field plate technique is diagramed in Figure 2

[10]. First demonstrated on GaAs HFETs, the field plate technique was first implemented on a GaN HEMT by Chini. This technique greatly reduced drain current dispersion, avoiding the 'knee walk-out' phenomena shown in Figure 3 as gate bias is increased [11].

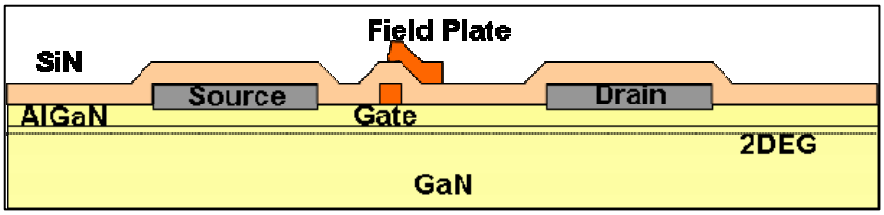

Figure 2. Field-Plated Device Structure[10]

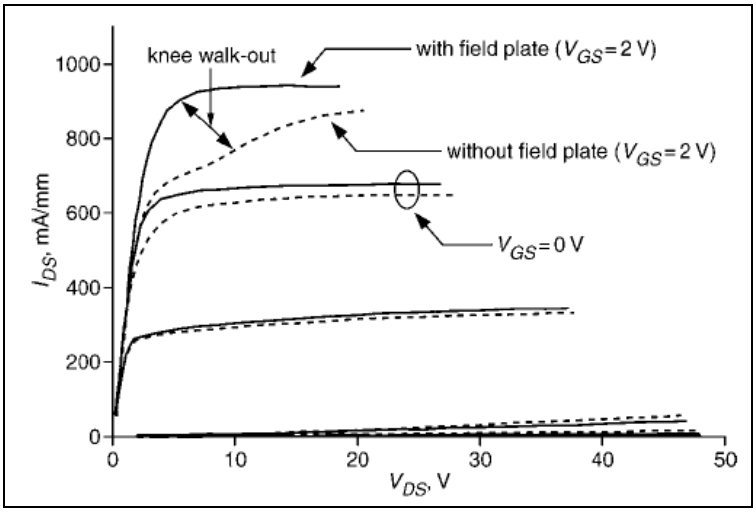

Figure 3. IV Characteristics Showing Knee Walk-Out [11]

III. DEVICE MODELING AND SIMULATION

A. SILVACO

The device simulation software package by Silvaco International was used to perform the modeling in this thesis work. Silvaco's ATLAS™ program performed the device structuring and subprogram calls while BLAZE2D/3D™ and GIGA™ performed specialized functions required for III-IV, heterojunction devices, and thermal modeling. The model parameters were programmed with DECKBUILD™ and the device parameters and graphics were extracted using TONYPLOT™ and TONYPLOT3D™.

The Silvaco software models a device in either two- or three-dimensional matrix-mesh format. Each mesh point represents a physical location within the modeled device and at that point, the program simulates transport properties via differential equations derived from Maxwell's equations. Numerical analysis is used to solve for electrostatic potential and carrier densities within the model. In addition to Poisson's equation, the continuity equations and the transport equations; the Lattice Heat Flow equation, listed in Appendix A, is added by using GIGA™. The heat generation term in the Lattice Heat Flow equation is further enhanced in this model by utilizing the Joule Heating function of GIGA™.

B. PRIOR THERMAL MODELING EFFORTS

Prior thermal modeling of GaN HEMTs with was performed by Kenneth Holmes in 2002 at the Naval Postgraduate School under the guidance of Todd Weatherford [3]. The model was also created using the Silvaco software suite. The model reported by Holmes was a modified model initially created by the Office of Naval Research and heavily modified by Karl Eimers using a novel piezoelectric subroutine within the existing model [4]. The thermal aspects of Holmes' model are inferred through electron concentration under bias conditions; thermal conductivities of semiconductor and substrate materials, thermal resistance and induced boundary conditions were neglected.

Another modeling effort available to this researcher was provided by Bob Cottle of Silvaco International. Mr. Cottle had developed a Silvaco model that closely

resembled the device reported by Khan et al [12]. The Khan model aided this researcher in developing the model reported in this work.

C. THIS EFFORT

This work is based on a physical device created and tested by S. Tzeng at the University of California – Berkeley. Figure 4 is a picture of the device created by UC Berkeley and Figure 5 is a TONYPLOT3D™ created image of the device.

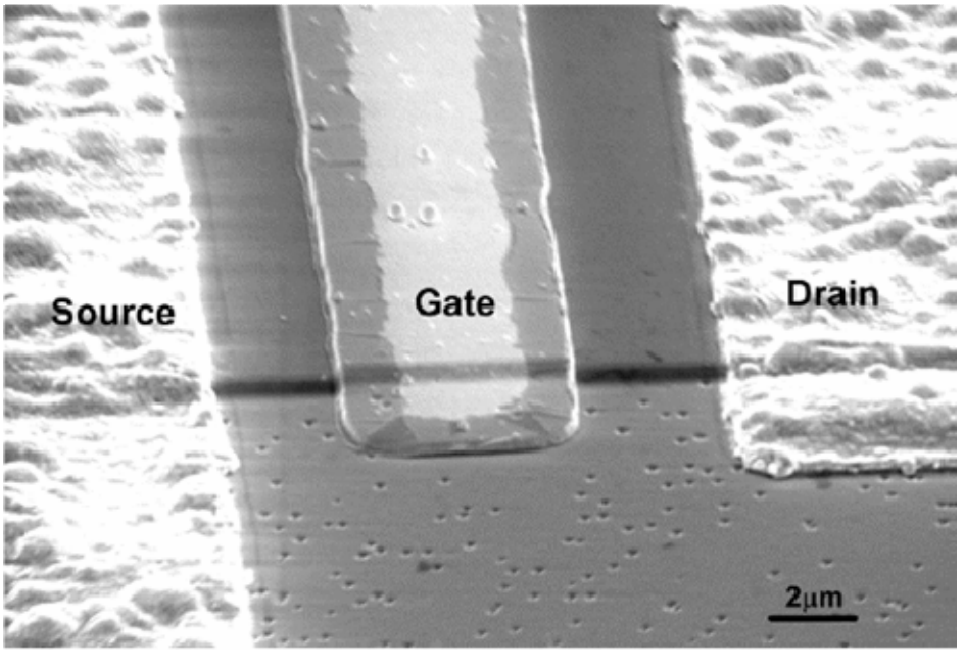

Figure 4. Scanning Electron Microscope (SEM) Image of GaN HEMT.[13]

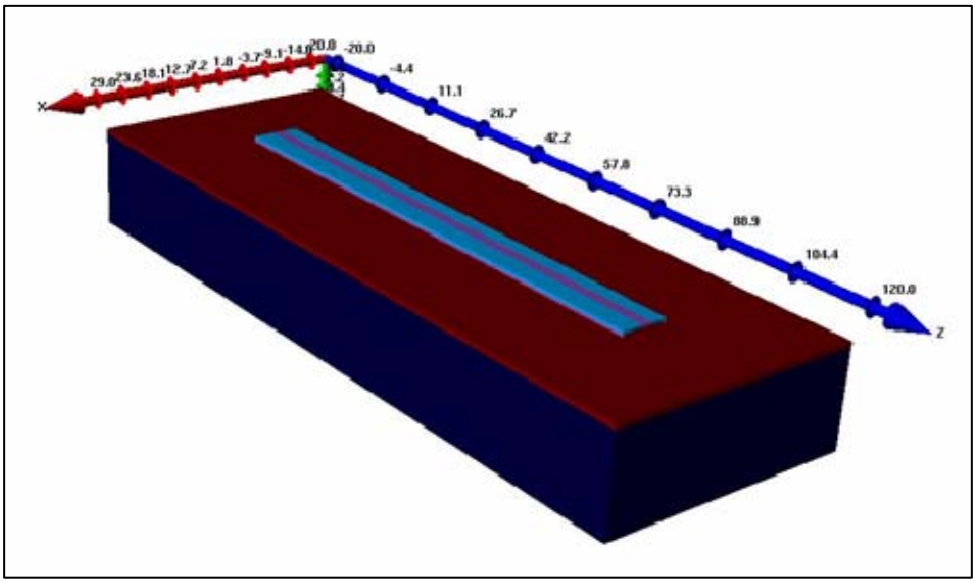

Figure 5. TONYPLOT3D™ Generated Image of Modeled GaN HEMT

1. Model Regions

The HEMT modeled in this work uses nine unique regions to represent the different materials and components of an actual physical HEMT device. Appendix B contains the text code used in the 2-dimensional model of the device created at UC – Berkeley. Figure 6 shows the regions of the model. Region 1, as listed in Appendix A, is the oxide region, silicon dioxide, which electrically isolates the gate, drain and source contacts. Regions 2-4 are the source, gate and drain electrodes, respectively. Region 5 is the AlGaN layer. This region vertically separates the gate contact from the GaN region and horizontally separates the source and drain contacts. The AlGaN is the top layer of the heterojunction that creates the 2DEG channel which is modulated by the gate bias during HEMT operation. Region 6 is an extremely thin layer of GaN directly below the AlGaN layer that also extends horizontally from source to drain. This thin GaN layer is used to simulate the 2DEG. A more detailed explanation of this region is found in the Model Development section. Regions 7 and 8 are the bulk GaN regions that vertically separate the contacts and heterojunction from the substrate material. Due to the 2-dimensional constraints and lattice-style computational nature of the Silvaco software, the bulk of the GaN region was constructed of two regions to accommodate the 90 degree angles of the source and drain contact edges. This building block style of construction was necessary for mathematical convergence of the model; this researcher learned 'the hard way' when trying to compile the model using other than 90 degree angles with the physical model construction. Region 9 is the substrate used for thermal management. Sapphire was the substrate used in the UC – Berkeley device. In the Results chapter of this work, diamond substrate is modeled and compared with the sapphire.

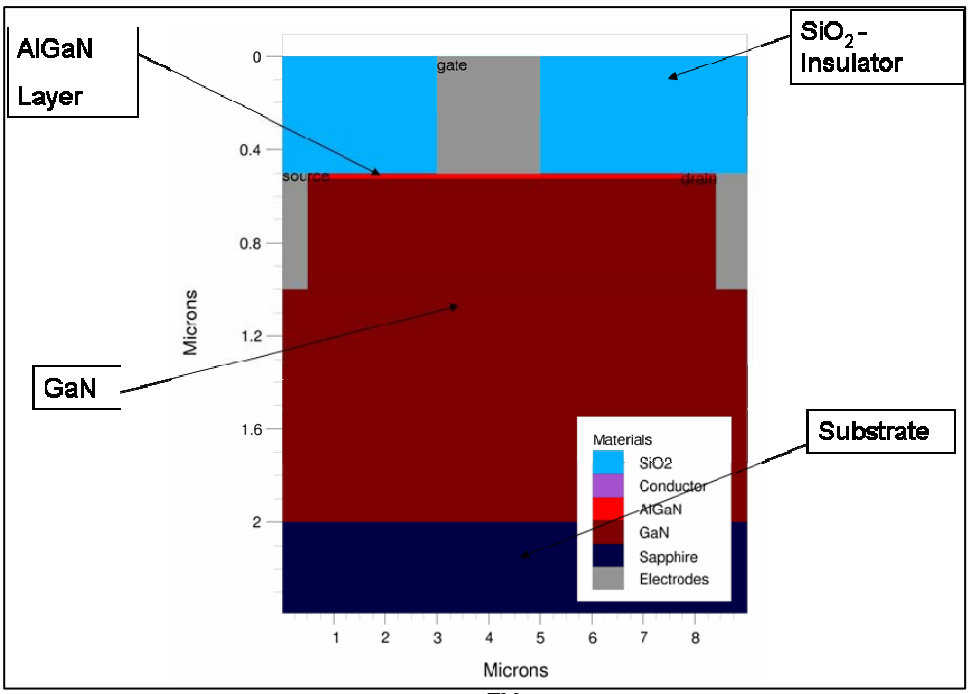

Figure 6. TONYPLOT™ View of Device Regions

2. Input File

The design and construction of this model was done using the DECKBUILD™ module within the Silvaco software suite. The code used to build the 3-dimensional model in this work is provided in Appendix C. Following is an explanation of the general sections of the input file code used to make the 3-D model created in this research.

The first section of the input file is Variable Definitions. This section comes after the call 'go atlas' is executed to enter the ATLAS™ module. In the Variable Definitions section, a number of useful user-defined variables are created to allow for easy changes to the physical dimensions of the model. This was quite useful when comparing different structure geometries as the model was changed throughout this research. For instance, changing the gate length from 1 micron to 2 microns required only one change to accomplish within the input file.

The Mesh Construction section of the input file allows for adding 'equation points' to the lattice mesh of equation points within the model. For instance, the level of detail and the number of individual points within the model is much greater within the

channel region than the substrate region. Figure 7 shows the lattice of 221,520 grid points created within the 3D model; the vector intersections define mesh points.

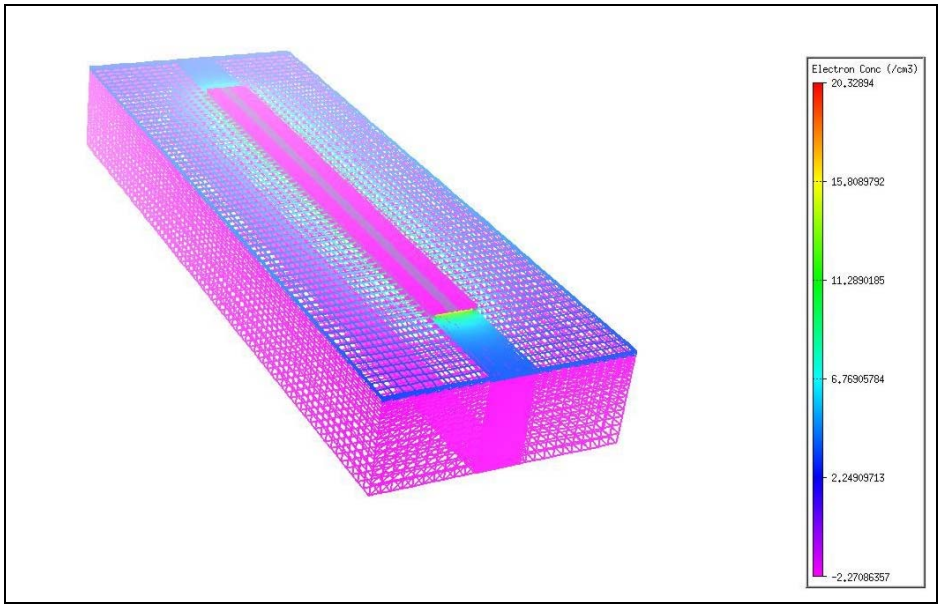

Figure 7. Lattice Mesh Rendering of Device Showing Electron Concentration

The Region Statements define areas within the mesh to have properties such as material type, doping levels, and compound composition percentages. This is the section where the device is built by assigning Cartesian-style corner points to each physical region of the device. Also, by assigning a material name to a region, a list of standard material properties is assigned to that region of the mesh. These properties can be further modified within the 'region' statement. More options are also available in next section.

The Modifying Statements section of the input file contains many function statements that allow for model adjustments. For example, the bandgap offset between the AlGaN/GaN heterojunction is not automatically accounted for and must therefore be modified for the model to be more realistic. Also in the Modifying Statements section is the 'interface charge' function where spontaneous polarization and piezoelectric effect are accounted for. Mobilities, saturation velocities, work functions, thermal boundaries and conductivities are assigned in this region. A very important function called 'models' is used in this section. 'Models' specifies which physical mechanisms are included in the

model calculations. It is here where the GIGA^{TM} functions involving lattice temperature and joule heating are called to be included in the model.

Lastly, the Output Statements region is used to 'bench test' the model by applying biases and displaying effects brought on by external sources. IV curves, electron concentrations, lattice temperatures and contact currents are examples of available outputs after the model solutions have been calculated using TONYPLOT^{TM} and TONYPLOT3D^{TM}. Structure and log files can be saved at successive bias points for tests such as step biasing and multiple curve generations.

3. Model Development

Several assumptions were made when creating the model. The boundary material used for the buffer layer between the sapphire substrate and the GaN is ignored. Ignoring this layer may have an effect on thermal management, but because a layer of similar buffer material would be used for a diamond or SiC substrate, comparing different substrates ignoring the buffer layer is reasonable. The bottom of the device, at the lowest point at the edge of the substrate, is a 'perfect heat sink' kept at 27 degrees Celsius.

Another assumption is the gate, drain and source contacts in the model are treated as perfect electrical conductors. Lastly, the interfaces between the layers were considered ideal with no modeled defects or surface modifications besides the interface charge to simulate the piezoelectric effect.

Starting with a model based on the Khan device, this researcher first attempted to create an electrically accurate 2-dimensional model of the device from UC - Berkeley. The Khan model was being used by Mr. Bob Cottle to more closely simulate the piezoelectric effect using the 'piezo' function of ATLAS^{TM} and comparing the results with a model using an interface charge. Mr. Cottle is a software developer at Silvaco International who had been working on modifying the ATLAS^{TM} code, specifically the 'piezo' function, when the Khan model was made available to this researcher. After several unsuccessful attempts by this researcher using the 'piezo' function to accurately model the electrical effects of a heterojunction, an interface charge was inserted at the AlGaN/GaN boundary. When combined with a thin GaN region of increased mobility directly below the AlGaN/GaN junction, the desired effect is achieved. One of the goals

of this research was to model the device in 3-dimensions and the 'piezo' function and prior piezoelectric modeling efforts such as Reference 4 are not available for use in 3-D models at the time of this writing; the interface charge was the only available solution.

Structuring the model to match the dimensional characteristics of the physical device was paramount. Such an approach seemed the most logical with the end goal to eventually use 3-dimensional thermal modeling. Starting from there, an accurate electrical model was created by varying the electron mobilities and saturation velocities of the AlGaN and GaN layers, donor concentration within the GaN and AlGaN regions, interface charge value and the gate work function. The values chosen were based on published data and refined through trial and error to achieve the best match of drain IV curves. The Results section of this work compares the model to the actual device in more detail.

The individual values that were most often modified throughout the model development were AlGaN layer thickness, Gate Work Function (WF), donor levels in AlGaN and GaN layers, the interface charge at the heterojunction and the electron mobilities and saturation velocities in each of the AlGaN and GaN layers. Early in the model development, the AlGaN layer thickness was given the most attention. In the work by Tzeng, no clear AlGaN layer thickness was evaluated as optimum, so a variety of layer thicknesses were modeled to determine which would give the closest electrical output characteristics to Tzeng's results. Eventually, the 267 angstrom thickness was chosen because AlGaN thickness did not have a notably strong effect on modeled device performance. Also, results for the most often referenced HEMT device of exact thickness given by Tzeng for the 0.28 Al mole fraction of AlGaN was the 267 angstrom device. Gate WF had the largest effect on device linearity and drain current over the modeled bias ranges plotted in the next section. This researcher decided to use a gate WF of 4.3 to coincide with the generally accepted WF of Aluminum when used as a gate contact for a FET. Generally accepted ranges of available extra electrons at the heterojunction for the piezoelectric and polarization effects of a GaN HEMT are around 10^{13} cm^{-2}. Therefore, an interface charge near that level was necessary to model the piezoelectric effect. The interface charge and donor levels, saturation velocities and electron mobilities within the semiconductor layers were the four values that this researcher changed most often to

achieve a final model that most closely resembled the actual device. The highest levels were naturally given to the 2 angstrom GaN layer directly below the heterojunction to simulate the 2DEG. Final values were chosen through trial and error until the most accurate representation of IV curves was achieved.

A third dimension to the model was included after the 2-dimensional model closely resembled the electrical characteristics of the Tzeng device. The gate width of the model is 100 microns with between 15 to 20 microns of GaN and sapphire substrate extending around the active region to allow for thermal spreading. A picture of a 3-D model showing localized heating of the HEMT on sapphire at a drain bias of 55 V is shown in Figure 8. The base of the substrate is fixed at 27°C and the maximum localized temperature in Figure 8 is 215°C.

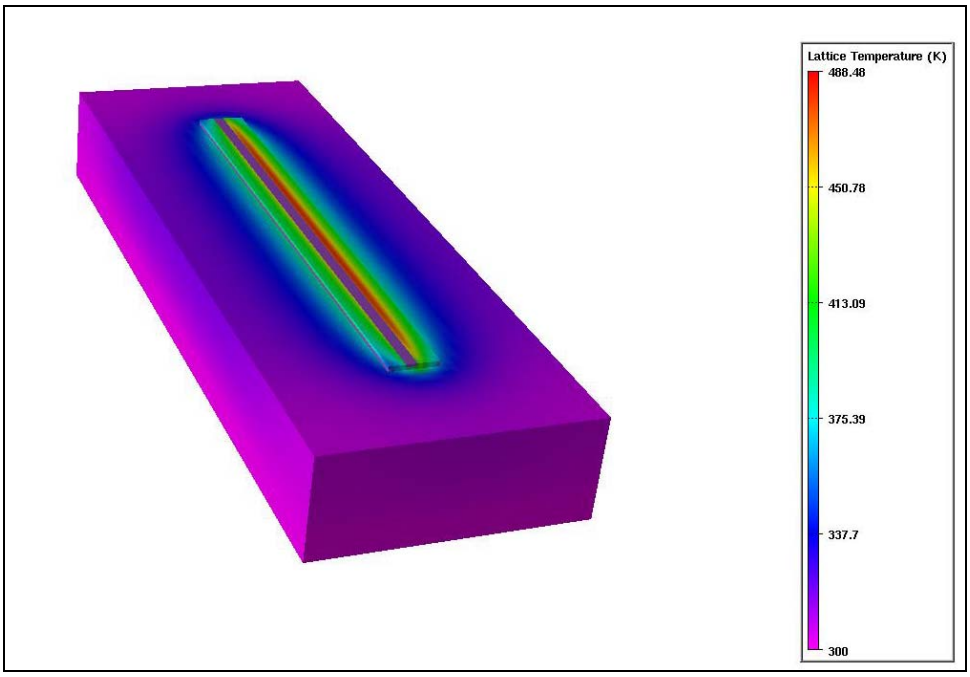

Figure 8. TONYPLOT3D™ Lattice Temperature View of HEMT on Sapphire

Through model development several notable discoveries were made based on intermediate simulation results. When the device drain is biased at 55 V, the layer of diamond required to properly cool the device to 27°C at the base of the substrate is 14 microns. Using thinner diamond substrates prevents the model engine from converging and displays much higher maximum channel temperatures while the simulation is

running when compared to a model that will converge with appropriate substrate thickness. Another discovery was that the GaN model layer could be as thin as 0.5 microns and the electrical results were identical over the same bias conditions reported by Tzeng. Thermal results were also identical over the same bias conditions when compared to the initial model with over 1.4 microns of GaN. Conditions at higher bias were not modeled during this research. One can postulate that decreasing the GaN layer will have multiple effects at higher bias conditions due to the depletion region necessary during device operation, but further research would have to be done to support this.

THIS PAGE INTENTIONALLY LEFT BLANK

IV. RESULTS

A. ELECTRICAL COMPARISON TO ACTUAL DEVICE

1. I_dV_d Curves

Figures 9 and 10 are the actual device and modeled device I_dV_d curves. Although not an exact match, the model shows remarkably similar trends in behavior as the gate is stepped and drain swept over the same voltages. Especially noteworthy is the 'dip', caused by negative differential resistance, in the topmost curve of each figure. Differential resistance is a physical effect caused by a varying effective mass at different velocities. Although not as linear as the measured results, the model output can be considered an electrical near match to the physical device and quite sufficient for modeling purposes especially considering the thermal nature of the remainder of this work.

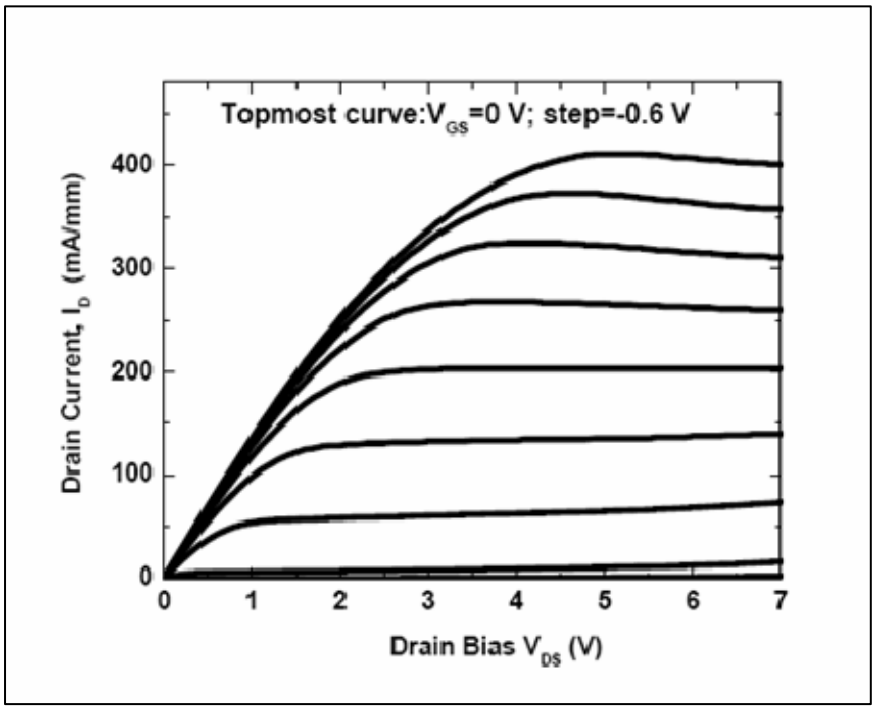

Figure 9. The Drain Current-Voltage Measurement of $Al_{0.28}Ga_{0.72}N$/GaN HEMT with Gate Length of 2 μm.[13]

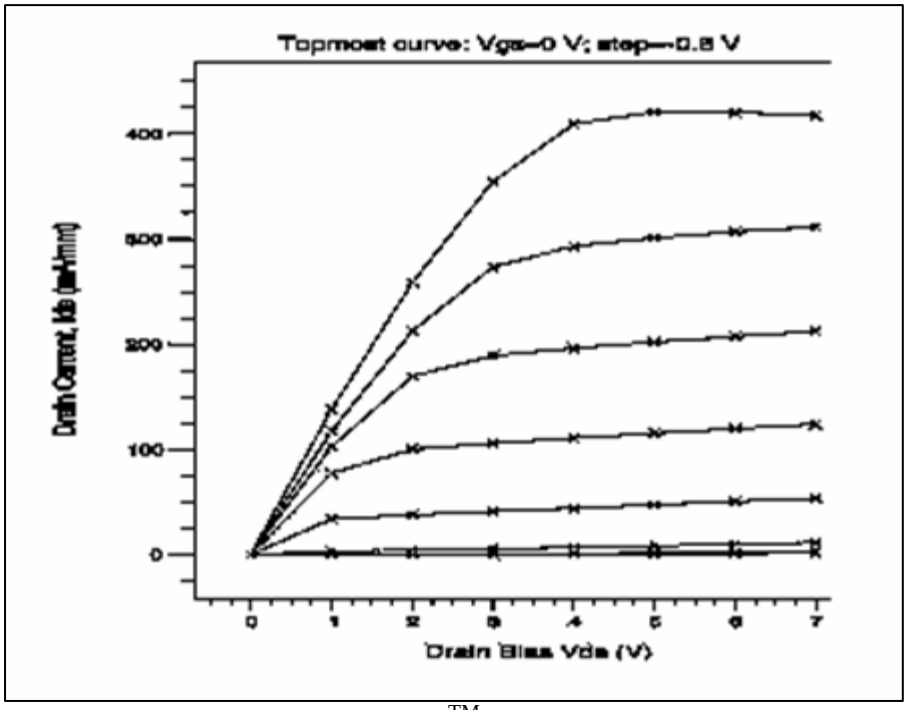

Figure 10. TONYPLOT™ Output of Drain IV Curve

2. I_gV_g Curves

Figures 11 and 12 are the actual device and modeled device I_gV_g curves. Each plot portrays the model and device with identical gate geometries. The sharp downward trend as the gate bias is swept through zero is similar in both plots. The gate current is off by many orders of magnitude; the ideal nature of the model shows a much lower gate leakage current. The model assumes zero defects at the AlGaN/GaN interface and zero trap defects in any of the materials used. Figures 9 and 11 are the only IV plots currently available of the device this research is modeled upon. Several GaN HEMTs created by UC – Berkeley of similar characteristics to those reported by Tzeng are being tested at NPS and will be the subject of further research.

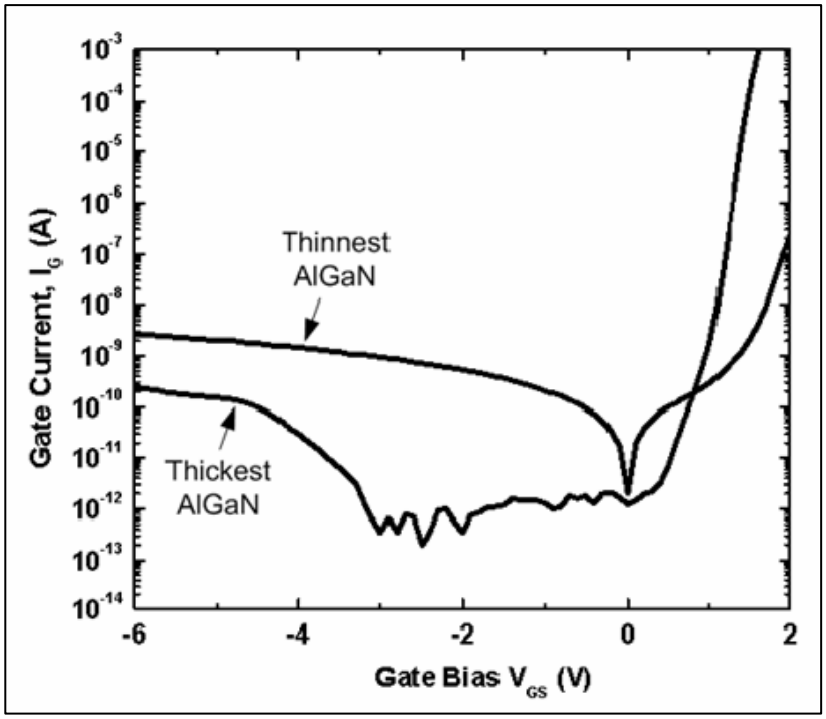

Figure 11. Gate Leakage Current of HEMT with Gate Length 2 µm and Gate Width 100 µm.[13]

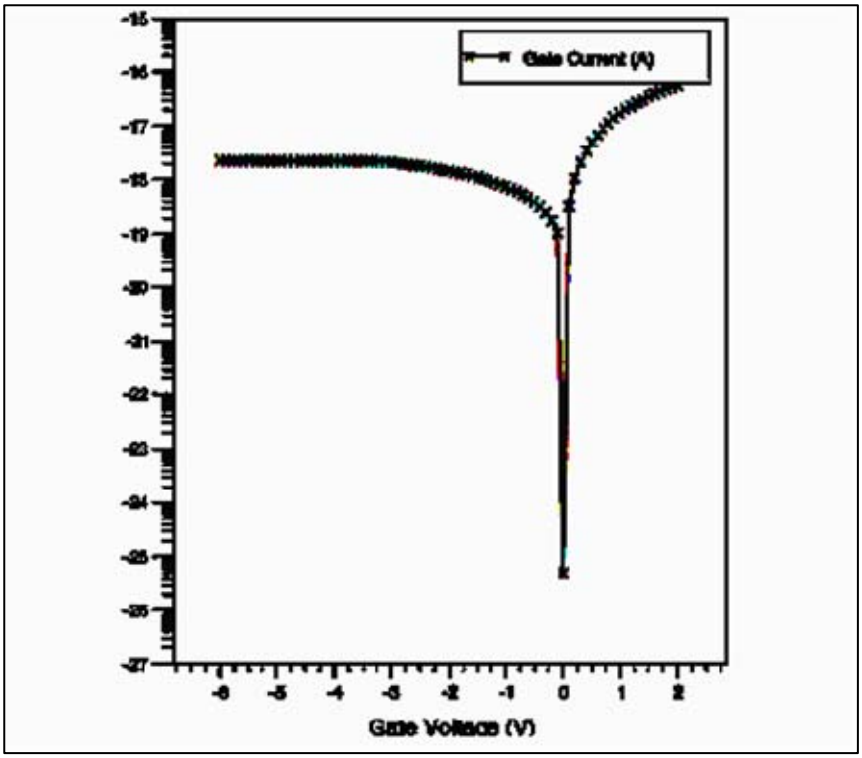

Figure 12. TONYPLOT™ Output of 3-D Sapphire Model Gate Leakage Current of with Gate Length 2 µm and Gate Width 100 µm.

B SUBSTRATE COMPARISONS

The models created in this work sought to match the electrical characteristics of the device created by Tzeng. After electrical similarity was achieved in a 2-dimensional model, the third dimension was added and the electrical results were identical over the ranges in Figures 9-12. The final simulation of this work compares changing the substrate material in the model from sapphire to diamond to show lower localized temperatures and increased device performance. When diamond was substituted in place of the sapphire in the 3-dimensional model, the model engine would not converge. Successful three-dimensional model run times were on the order of 15 hours per simulation on a 3 GHz dual-processor workstation. Non-convergence of models usually occurred around 35 minutes into the simulation. Reducing the number of grid points and removing the joule heating lattice temperature equations did not solve the convergence dilemma. Exhaustive model adjustment by this researcher did not produce a solution. The 2-dimensional model did not have a problem converging when diamond was used, nor was there any appreciable difference in electrical characteristics over the ranges in Figures 7-10 when compared to the device on sapphire. All heat comparisons are based on 2-dimensional simulations of sapphire versus diamond. The tests run by Tzeng did not include any record of temperatures while bias conditions were changed, so modeled temperatures cannot be correlated to actual data. NPS is currently testing GaN HEMT devices on sapphire over a range of temperatures. This will be reported in later research studies.

1. Electrical Differences

As stated above, there were no observable electrical differences between modeled devices when changing substrates over the electrical ranges tested on the physical device. When drain bias was brought up to ranges considered for device application, thermal effects dominated device performance. Figure 13 shows drain current performance of the modeled device with diamond and sapphire substrate material.

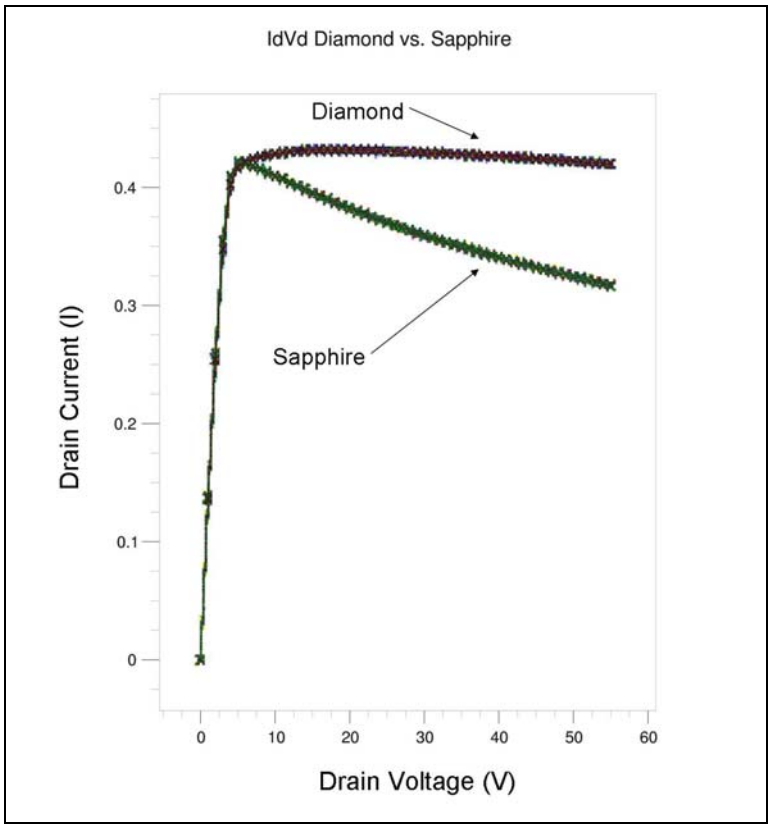

Figure 13. TONYPLOT^{TM} Generated IdVd Curves – Diamond vs. Sapphire

The modeled device on sapphire achieved a power output of approximately 16.5 W/mm while the device on diamond achieved approximately 22 W/mm with V_{gate}=0 V and V_{drain}=55 V. Gate leakage currents (see Figure 14) were on the order of 4 x 10^{-7} A on sapphire and 8 x 10^{-13} A on diamond. These output power results compare favorably with other recent GaN device research [8-11]. The thermal management properties of using diamond increased output power by 33% and decreased gate leakage by six orders of magnitude when compared to the same device modeled on sapphire.

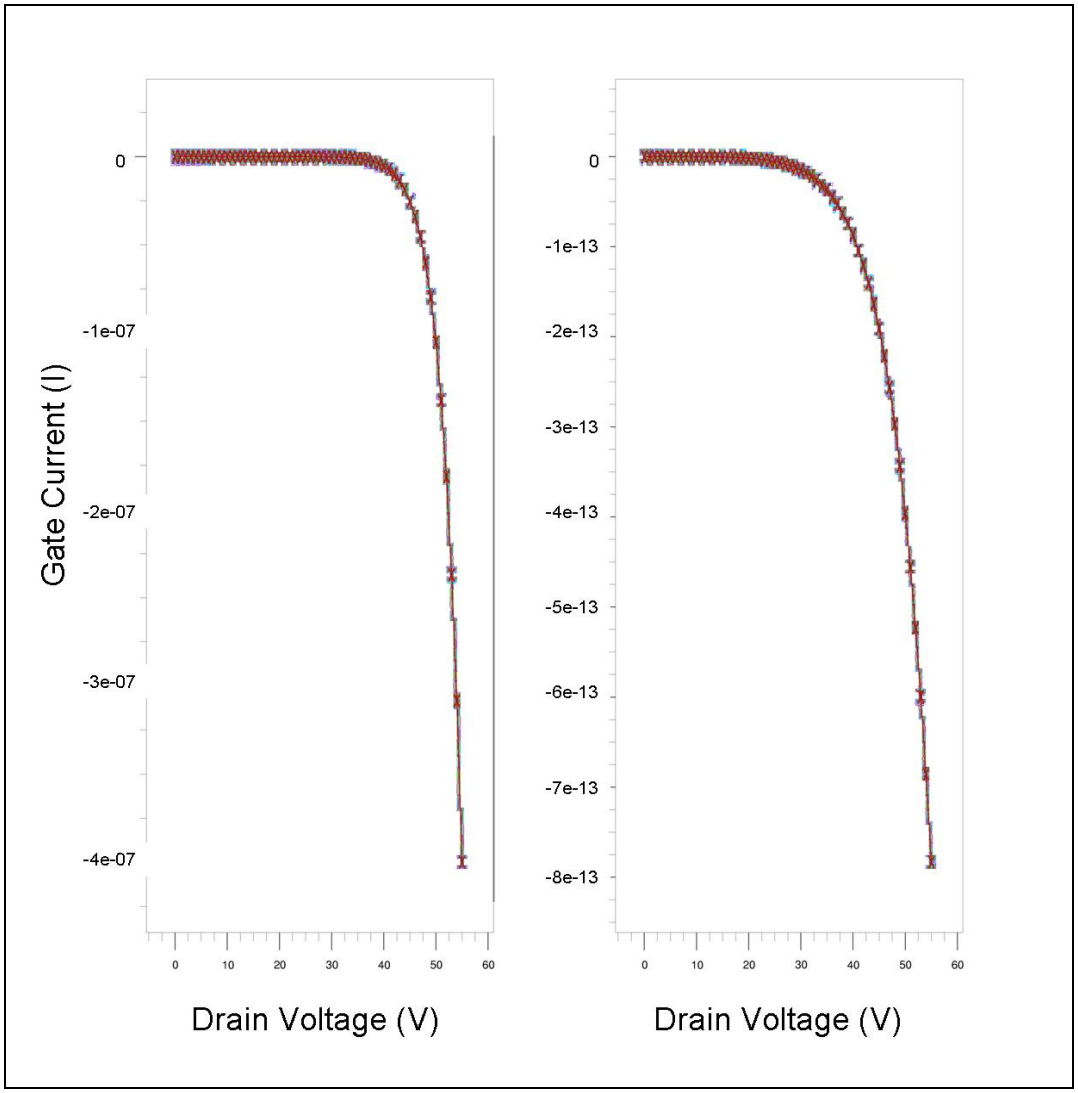

Figure 14. TONYPLOT™ of Gate Leakage Currents - Sapphire (left) vs. Diamond (right)

2. Thermal Differences

The maximum temperature of the modeled device on sapphire at 55 V drain bias was 319°C. The same device on diamond decreased the temperature to 148°C. These temperatures were observed on the same modeled device operating at 16.5 and 22 W/mm for sapphire and diamond with V_{gate}=0 V and V_{drain}=55 V. Drain currents are approximately 4 mA with the diamond substrate and 3 mA on sapphire (see Figure 13) each with a gate width of 100 microns. Gate leakage currents (see Figure 14) were on the order of 4 x 10^{-7} A on sapphire and 8 x 10^{-13} A on diamond. The difference in gate

leakage between the substrates may be attributed to the 171°C temperature difference. Figure 15 shows maximum localized heating occurred at the heterojunction almost directly below the gate on the drain side. This is consistent with actual device heating profiles.

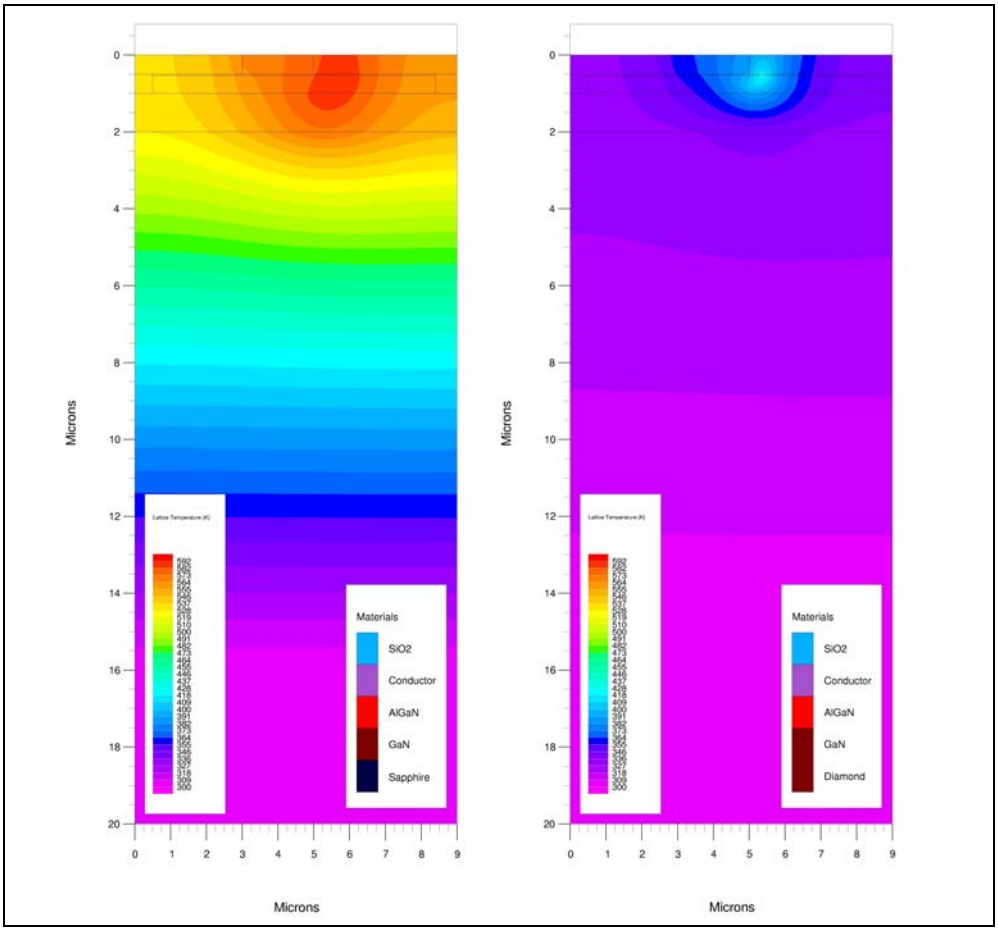

Figure 15. TONYPLOT™ of Sapphire (left) vs. Diamond (right) Substrate Comparison @ 55 V Drain Bias Condition.

THIS PAGE INTENTIONALLY LEFT BLANK

V. CONCLUSIONS AND RECOMMENDATIONS

A. CONCLUSIONS

An AlGaN/GaN HEMT model can accurately simulate an actual device over a similar range of measured bias conditions. Using IV plots, measured material characteristics and dimensions an accurate computer model of an AlGaN/GaN HEMT can be used to simulate extreme bias conditions, find estimated regions of highest heat generation and uncover bias conditions that gate leakage will occur without stressing an actual device. Furthermore, an accurate model can be used to show marked improvements in device performance and thermal management by replacing a sapphire substrate with diamond. Maximum device temperatures as predicted by the simulation can be reduced from 319°C to 148°C while performing under likely operating conditions. This temperature reduction leads to an immediate device output power increase of 33% and would lead to higher reliability and longer component lifetime without an input power increase.

Device temperature is directly related to reliability and lifetime. An often cited approach to predicting device median lifetimes is the Arrhenius Model for Temperature Dependence. [14]

$t_m(T) = A \cdot e^{E_A/kT}$ [Arrhenius Model for Temperature Dependence]

where:

E_A is Activation energy (eV)

A is a constant acceleration factor (dimensionless)

k is Boltzmann's constant (eV/°K)

Activation energies will typically range from 0.3 to 1.7 for GaN HEMTs. Given an acceleration factor (A) of 1 and E_A of 0.3 eV, a typical activation energy for a gate-related defect, and using the temperatures from the model output at 55 V gate bias, the expected lifetime of the device could be increased from 358 hours to 3903 hours by replacing the sapphire substrate with diamond; an order of magnitude increase can be expected in device lifetime at similar power levels.

Finally, the most promising conclusion is the output power of the modeled device compared to the theoretical approximation of GaN-on-diamond from Chapter Two Section B of this work. Filipov concluded that GaN-on-sapphire could achieve a 2.5 W/mm thermal dissipation performance and GaN-on-SiC 12.5 W/mm. The thermal conductivities of the sapphire and SiC are 1.7 and 4.9 W/cm•K, respectively. The value for diamond used for this research was conservatively chosen to be 10 W/cm•K. Assuming that thermal boundary resistance is proportional to substrate thermal conductivity given equal boundary interface quality, GaN-on-diamond could have a thermal dissipation performance over 20 W/mm. The output power of the model using a diamond substrate was approximately 22 W/mm. Based on findings in Reference 7 and the thermal conductivity values used in the model, the results of this work are in order of expectation.

B. RECOMMENDATIONS

Before electrical and noise characteristics can be accurately extracted from this model more work should be done to correctly utilize the 'piezo' function of ATLAS^{TM} within this model. Although the approach used by this researcher provided an excellent match to IV characteristics over the measured ranges, the small signal analysis and output given a high-frequency input could give inaccurate results. Relying on an ATLAS^{TM} function specifically built for the piezoelectric effect and using constant saturation velocities and electron mobilities over a contiguous device region would make for a more plausible model at high frequencies.

To provide a more accurate model from a thermal standpoint more data should be gathered from an actual device while under a variety of measured thermal conditions. This data could be correlated to modeled data and lead to the use of alternative thermal functions to provide a more accurate overall model. Another way to increase thermal accuracy would be to incorporate hot carrier effects into the model. This researcher avoided adding hot carrier effects due to the inordinate amount of time an individual simulation was taking to converge. By decreasing the amount of mesh points and simplifying the physical dimensions of the device (i.e., using linear electrical contacts and removing insulator regions), the model may converge in a more tolerable time frame

and more functions within ATLAS^{TM} could be incorporated. Boundary layer interface analysis for thermal conductivity could also be investigated.

The differences in device temperature at identical bias conditions between the 2-D and 3-D models of GaN-on-sapphire are dramatic. The 2-D model has a maximum localized temperature of 319°C while the 3-D model only 215°C. The increase in heat dissipation of the added dimension is very significant. Follow-on efforts should concentrate on solving the convergence problem when modeling with diamond.

The device modeled in this work was built and tested by S. Tzeng at UC Berkeley. Currently Dr. Petra Specht and her researchers at UC – Berkeley's Eicke Weber Group are striving to accurately grow Gallium Nitride layers directly on Diamond substrate material, as well as GaN on a several micron thin layer of silicon which has diamond grown on its backside. Based on the output power and thermal results from this research, such an accomplishment has the potential to revolutionize GaN device thermal management and provide the missing piece in device reliability that GaN-based devices require.

THIS PAGE INTENTIONALLY LEFT BLANK

APPENDIX A. EQUATIONS ADDED TO BASIC SILVACO MODEL

Following is a list of equations used by the various mathematical functions within the model. These equations were added specifically by this researcher in addition to the standard equations used within ATLAS™ to more accurately model the actual device. The heat related equations were the most significant additions to this research. The Lattice Heat flow equation, with inputs from the Thermal Conductivity equation and Heat Generation Equation, is solved at each mesh point along with five other physics equations based on Maxwell's laws to provide an accurate lattice temperature model output.

$$C\frac{\partial T_L}{\partial t} = \nabla(\kappa \nabla T_L) + H$$ [Lattice Heat Flow Equation]

$$\kappa(T) = 1/(A + B \times T + C \times T^2)$$ [Thermal Conductivity Equation]

$$H = \left[q\frac{\left|\overrightarrow{J_n}\right|^2}{\mu_n n} + q\frac{\left|\overrightarrow{J_p}\right|^2}{\mu_p p} \right]$$ [Heat Generation Equation using joule heating function]

$$\mu_n = \mu_{no}\left(\frac{T_L}{300}\right)^{-1.5}$$ [Mobility Equation]

$$\Delta E_C = (E_{AlGaN} - E_{GaN}) \cdot 0.65$$ [Heterostructure Bandgap alignment 65%]

where:

C is the heat capacitance per unit volume (F/cm^3)

κ is the thermal conductivity (W/cm·°K).

T_L is the local lattice temperature (°K).

$\overrightarrow{J_n}$ and $\overrightarrow{J_p}$ are the electron and hole current densities, respectively (carrier/cm^3).

μ_n is the material's electron mobility constant with units of cm^2/(V·s).

THIS PAGE INTENTIONALLY LEFT BLANK

APPENDIX B. 2-D DECKBUILD INPUT FILE

Following is the text code used for the 2-dimensional simulation of GaN on Sapphire:

```
go atlas

Title - 2D GaN on Sapph

######  VARIABLE DEFINITIONS ############

#  267 AlGaN layer default mobility MUN=1000/1620/1000 carr=1 WF=4.3

#   1e10 doping in all AlGaN & GaN layers IF charge=3.2e12

##############################


set devthk=20

set sourcegatespace=2

set gatedrainspace=3

set devwidth=4+$sourcegatespace+$gatedrainspace

set reg3xmin=$devwidth-1

set reg4xmin=1+$sourcegatespace

set reg4xmax=2+$reg4xmin

set reg5xmax=$devwidth-.5

set drainxmin=$devwidth-1

set drainxmax=$devwidth-.6

set ifchargemax=$devwidth-1.05

set WF=4.3


#  Set IV Limits
```

```
set vstart = 0

set vstop = 7

set vinc = 1



#####################  Mesh Construction ##############

mesh auto width=1000

x.m l=0.0 s=0.1

x.m l=0.5 s=0.1

x.m l=1.0 s=0.1

x.m l=$reg4xmin s=0.1

x.m l=$reg4xmax s=0.1

x.m l=$reg3xmin s=0.1

x.m l=$reg5xmax s=0.1

x.m l=$devwidth s=0.1

y.m l=0 s=0.5

y.m l=0.4 s=0.1

y.m l=0.49 s=0.005

y.m l=0.5 s=0.005

y.m l=0.525 s=0.005

y.m l=0.5267 s=0.00005

y.m l=0.5269 s=0.00005

y.m l=0.5270 s=0.005

y.m l=1.0 s=0.1
```

y.m l=2 s=0.5

y.m l=$devthk s=2.0

######################### Region Definitions ################

region num=1 mat=oxide x.min=0 x.max=$devwidth y.min=0 y.max=1

region num=2 mat=conductor x.min=0 x.max=.5 y.min=.5 y.max=1

region num=3 mat=conductor x.min=$drainxmax x.max=$devwidth y.min=.5 y.max=1

region num=4 mat=conductor x.min=$reg4xmin x.max=$reg4xmax y.min=0 y.max=0.5

region num=5 mat=AlGaN donors=1e10 x.comp=0.28 x.min=0.5 x.max=$reg5xmax y.min=0.5 y.max=0.5267

region num=6 mat=GaN donors=1e10 x.min=0.5 x.max=$reg5xmax y.min=0.5267 y.max=.5269

region num=7 mat=GaN donors=1e10 x.min=0.5 x.max=$reg5xmax y.min=0.5269 y.max=1

region num=8 mat=GaN donors=1e10 x.min=0 x.max=$devwidth y.min=1 y.max=2

region num=9 mat=Sapphire x.min=0 x.max=$devwidth y.min=2 y.max=$devthk

elec num=1 name=source x.min=0 x.max=0.5 y.min=0.5 y.max=1

elec num=2 name=drain x.min=$drainxmax x.max=$devwidth y.min=0.5 y.max=1

elec num=3 name=gate x.min=$reg4xmin x.max=$reg4xmax y.min=0 y.max=0.5

elec num=4 substrate

############## Modifying Statements ##################

```
interface charge=3.2e12 y.min=.51 y.max=.6 s.s

material mat=AlGaN align=.65

mobility region=5 mun=1000 vsatn=2e7
mobility region=6 mun=1600  vsatn=2.5e7
mobility region=7 mun=1000 vsatn=2.5e7
mobility region=8 mun=1000 vsatn=2e7

material mat=GaN tcon.polyn
material mat=AlGaN tcon.polyn
material mat=Sapphire tcon.polyn

models k.p print lat.temp joule.heat

contact name=gate work=$WF
thermcontact num=1 x.min=0 x.max=$devwidth y.min=14 y.max=$devthk temp=300
^boundary alpha=1.7

output con.band val.band charge
method gumits=300 clim.dd=1e5 autonr block carr=1

###################### Output Statements ##########
# idvd curves
```

```
solve
save outf=2D_SAP_g0.str
log outf=2dGaNsap_d_0.log
solve name=drain vdrain=$vstart vfinal=$vstop vstep=$vinc
save outf=2D_SAP_g0d7.str
log off
tonyplot 2dGaNsap_d_0.log -set IDVD.set
solve vdrain=0 vgate= -.6
save outf=solve_vgate-.6.str
log outf=2dGaNsap_d_1.log
solve name=drain vdrain=$vstart vfinal=$vstop vstep=$vinc
log off
solve vdrain=0 vgate= -1.2
save outf=solve_vgate-1.2.str
log outf=2dGaNsap_d_2.log
solve name=drain vdrain=$vstart vfinal=$vstop vstep=$vinc
log off
solve vdrain=0 vgate= -1.8
save outf=solve_vgate-1.8.str
log outf=2dGaNsap_d_3.log
solve name=drain vdrain=$vstart vfinal=$vstop vstep=$vinc
log off
solve vdrain=0 vgate= -2.4
save outf=solve_vgate-2.4.str
```

```
log outf=2dGaNsap_d_4.log

solve name=drain vdrain=$vstart vfinal=$vstop vstep=$vinc

log off

solve vdrain=0 vgate= -3

save outf=solve_vgate-3.str

log outf=2dGaNsap_d_5.log

solve name=drain vdrain=$vstart vfinal=$vstop vstep=$vinc

log off

solve vdrain=0 vgate= -3.6

save outf=solve_vgate-3.6.str

log outf=2dGaNsap_d_6.log

solve name=drain vdrain=$vstart vfinal=$vstop vstep=$vinc

log off

solve vdrain=0 vgate= -4.2

save outf=solve_vgate-4.2.str

log outf=2dGaNsap_d_7.log

solve name=drain vdrain=$vstart vfinal=$vstop vstep=$vinc

log off

tonyplot 2dGaNsap_d_0.log -overlay 2dGaNsap_d_1.log -overlay 2dGaNsap_d_2.log -overlay 2dGaNsap_d_3.log -overlay 2dGaNsap_d_4.log -overlay 2dGaNsap_d_5.log -overlay 2dGaNsap_d_6.log -overlay 2dGaNsap_d_7.log -set IDVD.set


# idvg curve

log outf=GaNsapp-gate_sweep.log
```

```
solve vdrain=0

solve name=gate vgate=0 vfinal=-4.2 vstep=.6

quit
```

THIS PAGE INTENTIONALLY LEFT BLANK

APPENDIX C. 3-D DECKBUILD INPUT FILE

Following is the text code used for the 3-dimensional simulation of GaN on Sapphire:

```
go atlas
Title - 3D GaN on Sapph
#         #########    VARIABLE DEFINITIONS      ############
#  267 AlGaN layer default mobility MUN=1000/1620/1000 carr=1 WF=4.3
#   1e14 doping in all AlGaN & GaN layers IF charge=3.2e12
################################
set AlGaNlayer=0.0267

set AlGaNdepth=.5+$AlGaNlayer
set GASdepth=$AlGaNdepth+0.0002
set GASmesh=$GASdepth+0.0002

set devthk=20
set sourcegatespace=2
set gatedrainspace=3

set devwidth=4+$sourcegatespace+$gatedrainspace

set reg3xmin=$devwidth-1
set reg4xmin=1+$sourcegatespace
```

```
set reg4xmax=2+$reg4xmin

set reg5xmax=$devwidth-.5


set drainxmin=$devwidth-1

set drainxmax=$devwidth-.6


set ifchargemax=$devwidth-1.05


set WF=4.3


#  Set IV Limits

set vstart = 0

set vstop = 7

set vinc = 1


######################## Mesh Construction ###########

mesh three.d

x.m l=-20 s=2

x.m l=-2 s=2

x.m l=0.0 s=0.2

x.m l=0.5 s=0.2

x.m l=1.0 s=0.2

x.m l=$reg4xmin s=0.2

x.m l=$reg4xmax s=0.2
```

x.m l=$reg3xmin s=0.2

x.m l=$reg5xmax s=0.2

x.m l=$devwidth s=0.2

x.m l=10 s=2

x.m l=29 s=2

y.m l=0 s=0.5

y.m l=0.4 s=0.1

y.m l=0.49 s=0.005

y.m l=0.5 s=0.005

y.m l=0.525 s=0.005

y.m l=$AlGaNdepth s=0.0001

y.m l=$GASdepth s=0.0001

y.m l=$GASmesh s=0.005

y.m l=1.0 s=0.1

y.m l=2 s=0.5

y.m l=$devthk s=2.0

z.m l=-20 s=2

z.m l=120 s=2

############### Region Statements #################

region num=1 mat=oxide x.min=0 x.max=$devwidth y.min=0 y.max=1 z.min=0 z.max=100

region num=2 mat=conductor x.min=0 x.max=.5 y.min=.5 y.max=1 z.min=0 z.max=100

region num=3 mat=conductor x.min=$drainxmax x.max=$devwidth y.min=.5 y.max=1 z.min=0 z.max=100

region num=4 mat=conductor x.min=$reg4xmin x.max=$reg4xmax y.min=0 y.max=0.5 z.min=0 z.max=100

region num=5 mat=AlGaN donors=1e10 x.comp=0.28 x.min=0.5 x.max=$reg5xmax y.min=0.5 y.max=$AlGaNdepth z.min=0 z.max=100

region num=6 mat=GaN donors=1e10 x.min=0.5 x.max=$reg5xmax y.min=$AlGaNdepth y.max=$GASdepth z.min=0 z.max=100

region num=7 mat=GaN donors=1e10 x.min=0.5 x.max=$reg5xmax y.min=$GASdepth y.max=1 z.min=0 z.max=100

region num=8 mat=GaN donors=1e10 x.min=-20 x.max=29 y.min=1 y.max=2 z.min=-20 z.max=120

region num=9 mat=Sapphire x.min=-20 x.max=29 y.min=2 y.max=$devthk z.min=-20 z.max=120

elec num=1 name=source x.min=0 x.max=0.5 y.min=0.5 y.max=1 z.min=0 z.max=100

elec num=2 name=drain x.min=$drainxmax x.max=$devwidth y.min=0.5 y.max=1 z.min=0 z.max=100

elec num=3 name=gate x.min=$reg4xmin x.max=$reg4xmax y.min=0 y.max=0.5 z.min=0 z.max=100

elec num=4 substrate

################ Modifying Statements ##############

interface charge=3.2e12 y.min=.51 y.max=.6 s.s

material mat=AlGaN align=.65

mobility region=5 mun=1000 vsatn=2e7

mobility region=6 mun=1600 vsatn=2.5e7

mobility region=7 mun=1000 vsatn=2.5e7

mobility region=8 mun=1000 vsatn=2e7

```
material mat=GaN tcon.polyn

material mat=AlGaN tcon.polyn

material mat=Sapphire tcon.polyn

models k.p print lat.temp joule.heat

contact name=gate work=$WF

thermcontact num=1 y.min=14 y.max=$devthk temp=300 ^boundary alpha=1.7

output con.band val.band charge

method gumits=300 clim.dd=1e5 autonr block carr=1

solve


############### Output Statements ###############

# idvd curves

save outf=3D_SAP_g0_d0.str

log outf=3dGaNsap_d_0.log

solve name=drain vdrain=$vstart vfinal=$vstop vstep=$vinc

save outf=3D_SAP_g0d7.str

log off

tonyplot 3D_SAP_g0d7.log -set IDVD.set

solve vdrain=0 vgate= -.6

save outf=solve_vgate-.6.str

log outf=3dGaNsap_d_1.log

solve name=drain vdrain=$vstart vfinal=$vstop vstep=$vinc

log off

solve vdrain=0 vgate= -1.2
```

```
save outf=solve_vgate-1.2.str
log outf=3dGaNsap_d_2.log
solve name=drain vdrain=$vstart vfinal=$vstop vstep=$vinc
log off
solve vdrain=0 vgate= -1.8
save outf=solve_vgate-1.8.str
log outf=3dGaNsap_d_3.log
solve name=drain vdrain=$vstart vfinal=$vstop vstep=$vinc
log off
solve vdrain=0 vgate= -2.4
save outf=solve_vgate-2.4.str
log outf=3dGaNsap_d_4.log
solve name=drain vdrain=$vstart vfinal=$vstop vstep=$vinc
log off
solve vdrain=0 vgate= -3
save outf=solve_vgate-3.str
log outf=3dGaNsap_d_5.log
solve name=drain vdrain=$vstart vfinal=$vstop vstep=$vinc
log off
solve vdrain=0 vgate= -3.6
save outf=solve_vgate-3.6.str
log outf=3dGaNsap_d_6.log
solve name=drain vdrain=$vstart vfinal=$vstop vstep=$vinc
log off
```

solve vdrain=0 vgate= -4.2

save outf=solve_vgate-4.2.str

log outf=3dGaNsap_d_7.log

solve name=drain vdrain=$vstart vfinal=$vstop vstep=$vinc

log off

tonyplot 3dGaNsap_d_0.log -overlay 3dGaNsap_d_1.log -overlay 3dGaNsap_d_2.log -overlay 3dGaNsap_d_3.log -overlay 3dGaNsap_d_4.log -overlay 3dGaNsap_d_5.log -overlay 3dGaNsap_d_6.log -overlay 3dGaNsap_d_7.log -set IDVD.set

idvg curve

log outf=GaNsapp3d-gate_sweep.log

solve vdrain=0

solve name=gate vgate=0 vfinal=-4.2 vstep=.6

quit

THIS PAGE INTENTIONALLY LEFT BLANK

LIST OF REFERENCES

1. Borges, Ricardo, “High Electron Mobility Transistors (HEMT).” internet, www.nitronex.com/education/ganHEMT.pdf, December 2005.

2. Eimers, Karl P. “2-D Modeling of GaN HEMTs Incorporating the Piezoelectric Effect.” Master’s Thesis, Naval Postgraduate School, Monterey, California, 2001.

3. Holmes, Kenneth L. “Two-Dimensional Modeling of Aluminum Gallium Nitride.” Master’s Thesis, Naval Postgraduate School, Monterey, California, 2002.

4. Kayali, S. et. al., “GaAs MMIC Reliability Assurance Guideline for Space Applications.” *JPL Publication 96-25*, pp. 39-43. Jet Propulsion Laboratory, Pasadena, California, 1996.

5. Edwards, A. P., J. A. Mittereder, S. C. Binari, D. S. Katzer, D. F. Storm, and J. A. Roussos. “Improved Reliability of AlGaN-GaN HEMTs Using an NH/sub 3/ Plasma Treatment Prior to SiN Passivation.” *Electron Device Letters, IEEE* 26, no. 4TY - JOUR (2005): 225-227.

6. Xing, H. et al., “Gallium Nitride Based Transistors.” *J. Phys.: Condens. Matter* 13 - JOUR (2001):7139-7157.

7. Filipov, K. A., and Balandin, A. A., “The Effect of the Thermal Boundary Resistance on Self-Heating of AlGaN/GaN HFETs.” *MRS Internet J. Nitride Semicond. Res.* 8, no. 4 - JOUR (2003): 1-4.

8. Mishra, U. K., P. Parikh, and Y. -F Wu. “AlGaN/GaN HEMTs-An Overview of Device Operation and Applications.” *Proceedings of the IEEE* 90, no. 6TY - JOUR (2002): 1022-1031.

9. Xu, H., N. K. Pervez, P. J. Hansen, L. Shen, S. Keller, U. K. Mishra, and R. A. York. “Integration of Ba/sub x/Sr/sub 1-x/TiO/sub 3/ Thin Films with AlGaN/GaN HEMT Circuits.” *Electron Device Letters, IEEE* 25, no. 2TY - JOUR (2004): 49-51.

10. Xu, H., C. Sanabria, S. Heikman, S. Keller, U. K. Mishra, and R. A. York. “High Power GaN Oscillators Using Field-Plated HEMT Structure.” (2005): 1345-1348.

11. Chini, A., D. Buttari, R. Coffie, S. Heikman, S. Keller, and U. K. Mishra. “12 W/mm Power Density AlGaN/GaN HEMTs on Sapphire Substrate.” *Electronics Letters* 40, no. 1TY - JOUR (2004): 73-74.

12. Khan, M. A., X. Hu, G. Sumin, A. Lunev, J. Yang, R. Gaska, and M. S. Shur. “AlGaN/GaN Metal Oxide Semiconductor Heterostructure Field Effect Transistor.” *Electron Device Letters, IEEE 21*, no. 2TY - JOUR (2000): 63-65.

13. Tzeng, Suzie, “Low-Frequency Noise Sources in III-V Semiconductor Heterostructures.” Ph.D. Diss., University of California – Berkeley, 2004.

14. Jensen, Finn, *Electronic Component Reliability*, John Wiley & Sons, Inc., New York, 1995, p. 205.

INITIAL DISTRIBUTION LIST

1. Defense Technical Information Center
   Ft. Belvoir, Virginia

2. Dudley Knox Library
   Naval Postgraduate School
   Monterey, California

3. Engineering and Technology Curricular Office, Code 34
   Naval Postgraduate School
   Monterey, California

4. Chairman, Code EC (590)
   Department of Electrical and Computer Engineering
   Naval Postgraduate School
   Monterey, California

5. Prof. Todd R. Weatherford, Code EC (590)/Wt
   Department of Electrical and Computer Engineering
   Naval Postgraduate School
   Monterey, California

6. Andrew A. Parker, Code EC (590)/Pk
   Department of Electrical and Computer Engineering
   Naval Postgraduate School
   Monterey, California

7. Dr. Petra Specht
   Materials Science & Engineering
   University of California, Berkeley at LBNL
   Berkeley, California

8. Jerry Zimmer
   SP3 Diamond Technologies
   2200 Martin Avenue
   Santa Clara, California

9. LT Roman P. Salm, USN
   Marina, California